

Supplemental Materials

Nanoscale Organization of Tetraspanins during HIV-1 budding by correlative dSTORM/AFM

Selma Dahmane^{1*}, Christine Doucet^{1*}, Antoine Le Gall¹, Célia Chamontin², Patrice Dosset¹, Florent Murcy¹, Laurent Fernandez¹, Desirée Salas Pastene¹, Eric Rubinstein^{3,4}, Marylène Mougel², Marcelo Nollmann¹, Pierre-Emmanuel Milhiet^{1#}

¹ Centre de Biochimie Structurale (CBS), INSERM, CNRS, Univ Montpellier

² IRIM, CNRS, University of Montpellier, Montpellier, France

³ Inserm, U935, Villejuif, France

⁴ Université Paris Sud, Institut André Lwoff, Villejuif, France

to whom correspondence should be addressed

* These two authors equally contributed to the work.

MATERIALS AND METHODS

Plasmids and antibodies

The codon-optimized untagged Gag and Gag-GFP constructs have been previously described ^{1,2}. Full length mAbs raised against CD81 (TS81), CD9 (SYB-1) and CD46 (11C5), were labeled with Alexa647 as previously described ³. Anti-GM130 was purchased from Sigma. Secondary antibodies were from Molecular Probes.

Cell culture and sample preparation

HeLa cells were grown in DMEM (Gibco) supplemented with 10% FCS (Gibco). For imaging, cells were seeded on 25 mm round glass coverslips placed in 6-well plates ($2 \cdot 10^5$ cells/well) (Marienfeld). Prior to use, coverslips were rinsed with acetone, ethanol, and water, then sonicated in 1M KOH for 20-30 minutes in a water bath. Coverslips were then extensively rinsed in MilliQ water, air-dried and plasma-cleaned for 20 minutes. They were then coated with collagen. Before transfection, cells were placed in fresh medium. Cells were transfected using 2 μ g DNA per well with an equimolar ratio of Gag-GFP and Gag. Cells were placed in fresh medium 4-6 hours after transfection and analysed 24-48h post-transfection. For immunostaining, cells were incubated for 15min at 37°C with Alexa647-conjugated primary antibody (1.5 μ g/mL), washed and fixed with 4% paraformaldehyde and 0.2% glutaraldehyde in PBS for 20 min at room temperature (fixation increases the membrane spring constant and thus facilitate AFM imaging). After fixation, cells were washed with PBS and incubated for 10min with 1/1000 dilution of 100 nm fluorescent beads emitting at four wavelengths (TetraSpeck Microspheres, Invitrogen) used as fiducial marks. For dSTORM imaging, an oxygen-scavenging PBS-based buffer included 10% glucose, 0.04 mg/mL glucose oxidase, and 0.5 mg/mL catalase, supplemented with 25 mM mercaptoethylamine (MEA) (all from Sigma).

For immunofluorescence, cells were washed with PBS, fixed with 4% PFA, and permeabilized in PBS with 1mg/mL BSA and 0.05% saponin. Cells were then incubated with anti-CD9 or anti-CD81 (1.5 μ g/ml) + anti-GM130 (1/300) in PBS + 1mg/ml BSA, rinsed with PBS and incubated with anti-mouse A647 (1/2000) + anti-rabbit A568 (1/2000) for 1h. Finally, cells were rinsed in PBS then water, mounted on glass slides with Vectashield (VectorLabs) and nailpolish. Images were acquired on a confocal microscope (SP8, Leica).

Image acquisition on AFM-SMLM Correlative Microscope

The setup was built as a combination of a Nanowizard 3 microscope (JPK, Berlin) together with a homemade objective-type TIRF inverted optical microscope (Zeiss, Le Pecq, France) equipped for single molecule localization microscopy with an oil-immersion objective (Plan-Apochromat 100x, 1.4

DIC, Zeiss). A 1.5x telescope was used to obtain a final imaging magnification of 150-fold corresponding to a pixel size of 107 nm. Four lasers were used for excitation/photo-activation: 405 nm (OBIS, LX 405-50, Coherent Inc.), 488 nm (OBIS, LX 488-50, Coherent Inc.), 561 nm (OBIS, LX 561-50, Coherent Inc.), and 640 nm (OBIS, LX 640-100, Coherent Inc.). Laser lines were expanded, and coupled into a single beam using dichroic mirrors (427, 552 and 613 nm laser MUXTM, Semrock). An acousto-optic tunable filter (AOTFnc-400.650-TN, AA opto-electronics) was used to modulate laser intensity. Two achromatic lenses were used to expand the excitation laser and an additional dichroic mirror (zt405/488/561/638rpc, Chroma) to direct it towards the back focal plane of the objective. Fluorescence light was spectrally filtered with emission filters (ET525/50m, ET600/50m and ET700/75m, Chroma Technology) and imaged on an EMCCD camera (iXon Ultra897, Andor Technologies). The microscope was equipped with a piezo Tip Assisted Optics (TAO) module (JPK, Berlin) allowing 100x100x10 μm sample displacement in x, y and z direction, respectively.

To ensure the stability of the focus during acquisition, home-made autofocus system was built. 4% of the red laser was deviated from the optical path using a glass plate and directed at the sample/glass coverslip interface. This beam was then reflected towards the objective lens and redirected following the same path as the incident beam and guided to a home-made QPD allowing its transverse displacements to be detected and corrected by the TAO stage. Camera, lasers and filter wheel were controlled with a software written in LABVIEW (National Instruments).

For dSTORM acquisitions, two lasers were used to illuminate the cells. 1 kW/cm^2 of 641 nm laser illumination was used for imaging and $0\text{-}0.1\text{ kW/cm}^2$ of 405 nm for conversion from the dark state. The 641nm laser continuously illuminated the sample during data acquisition, while the activation laser was pulsed for 50ms. The intensity of activation was progressively increased throughout the acquisition to ensure a constant amount of simultaneously activated fluorophores within the labeled structures. For image acquisition, on average 25,000 frames were recorded at a rate of 50 ms/frame. Cells were further imaged with AFM after replacement of the dSTORM oxygen-scavenging buffer by PBS. AFM imaging was performed with a Nanowizard 3 (JPK Berlin, Germany) using the Quantitative

Imaging mode with MLCT cantilevers (Nano-Bruker, Palaiseau, France). To achieve the best combination between AFM and fluorescence images, we used the built-in software calibration DirectOverlay™ which is using the accuracy of the AFM closed loop scanning system enabling the overlay of both microscopies at high resolution precision, typically 10 to 30nm.

dSTORM data processing and analysis

Post-acquisition image analysis was performed using the Multiple Target Tracking (MTT) algorithm described elsewhere ⁴ generating tables containing the x-y particle coordinates of each molecule detected during the acquisition. Lateral drift correction was performed as described previously by following the trajectory of the fiducial marks and employing custom software PALMcbcs written in MATLAB (MathWorks)⁵. The experimental drift correction precision was typically 3-10 nm.

Clusterization analysis was done by a tessellation approach using a modified version of the Voronoi tessellation algorithm developed by Levet et al. ⁶. Single-molecule localizations are first converted into a Voronoi diagram. Briefly 10um x 10um regions of interest (ROI) were selected randomly in central regions of the cells and Voronoi diagrams were retrieved using the 'voronoi' function. Local densities were calculated as the inverse value of the corresponding voronoi cells area. For each ROI, a density histogram of experimental localizations was generated and compared to the density histogram of an equivalent number of randomly distributed localizations. The histograms intersection defined a threshold D. Localizations were considered to be clustered when exhibiting a local density $d > 1.6D$.

A binary map of clustered localizations was generated and localization clusters were then segmented. A mask was created, based on GFP fluorescence, to define areas corresponding to Gag assembly sites. Using this mask, clusters were sorted depending on their co-localization with Gag. Clusters areas were then calculated for clusters within or outside Gag assembly sites. All analyses were carried out in Matlab. Graphical representations and statistical analyses were performed using Prism.

AFM data processing and analysis

The distances between CD9 localizations and the plasma membrane were measured using homemade Matlab-based program. Briefly, the AFM, Gag-GFP and CD9 dSTORM images were overlapped in Matlab by scaling the pixel sizes. Based on the AFM image, we determined the coordinates of the centers and the tips of the buds, and a segment lining the plasma membrane. We then selected CD9 localizations within a radius of 200 nm from the buds centers. The distances of all selected localizations to the segment were calculated and divided by the tip to plasma membrane distance. Relative CD9 to plasma membrane distances were compiled for 12 buds and a distribution histogram was built in Matlab.

To calculate the density of CD9 clusters (number of localization events) within Gag-GFP assembly sites and buds from AFM images, we measured the surface corresponding to the topography probed by the AFM tip using Delaunay triangulation.

FACS

48h post-transfection, cells were trypsinized and rinsed twice in cold PBS. Cells were then incubated with appropriate antibodies diluted in PBS +3% serum at 1.5 µg/mL for 30 minutes on ice. Cells were rinsed in PBS + 3% serum and incubated with Alexa647 anti-Mouse (Molecular Probes) for 30 minutes on ice. Cells were then rinsed in cold PBS, fixed in 4%PFA for 10 minutes at room temperature, and rinsed twice in cold PBS. FACS analysis was carried out on a MACSQuant analyzer (Miltenyi). All data were acquired using the same detector settings and gating parameters. Data were analyzed with FlowJo and the ratio of tetraspanin levels in transfected (GFP+ or GFP++) / untransfected (GFP-) cells were calculated. Data were averaged from 4 independent experiments.

Quantitation of VLP production in HeLa cells depleted or not of CD9 and CD81

HeLa cells were seeded in 6 well plates and co-transfected with 1µg of pNL4-3ΔEnv, 1µg pMaYFP-ΔEnv and 100pmol siRNA (either, scrambled or against CD9 and/or CD81). 48h after transfection, culture supernatants were collected and submitted to ultracentrifugation at 30,000g for 90 minutes on a sucrose cushion. Pellets were resuspended in 40µl of DMEM without serum and stored at -80°C

until SDS-PAGE analysis. Cells were scraped on ice and pelleted. Each pellet was resuspended in 100ul of TNE-Triton (10mM Tris pH7.5, 150mM NaCl, 5mM EDTA, 1% Triton), complemented with protease inhibitor cocktail (EDTA-free Complete, Roche) and incubated on ice for 10 minutes, vortexing 2-3 times. Lysates were spun for 10 minutes at 11,000g; supernatants were collected and stored at -80°C until SDS-PAGE analysis.

CD9, CD81 and p24 contents in both cell extract and supernatant were analyzed by western blotting using anti-tetraspanin antibodies described above and anti-p24 antibodies (Serotec), revealed by peroxidase-conjugated goat anti-mouse antibodies from Jackson ImmunoResearch. Quantitation of western-blotting signals was performed with FIJI.

Silencing RNA oligonucleotides were from Ambion: Oligo sc (UAGAUACCAUGCACAAAUCC dTdT), siCD9 (GCAGAAATCCTGCAATGAAAdTdT) and siCD81 (CACGUCGCCUUAACU GUAdTdT).

FIGURE LEGENDS

Figure S1 - dSTORM cluster analysis of CD9 in HeLa cells

(A) Localization accuracy: frequency distributions of dSTORM localization precision in HeLa cells under naive (WT, number of cells = 19), 24h (number of cells = 17) or 48h (number of cells = 21) Gag-GFP expression.

(B) Gag-GFP fluorescence signal acquired by TIRF microscopy from HeLa cells expressing HIV-1 Gag-GFP for 24h or 48h (shown in Fig. 1A). Scale bars, 10 μ m.

(C) Left: TIRF image of Gag-GFP foci at the plasma membrane of a HeLa cells 48h post-transfection (left); relative GFP intensity is pseudo-colored according to the associated color scale bar (arbitrary units). Right: the corresponding molecular density map of CD9-Alexa647; density is pseudo-colored according to the associated color scale.

D) Normalized CD9 density (ratio of molecular density of CD9 within Gag-GFP domains to total molecular density) correlated to the normalized intensity of Gag-GFP assembly sites (48h post-transfection, number of cells = 8). The correlation coefficient is 0.44 with a r^2 of 0.33.

E) Box and Whiskers representation (5-95% percentile) of areas depleted of CD9 clusters calculated from dSTORM analysis in control cells (red) or in cells expressing Gag-GFP proteins 24h (blue) or 48h (green) after transfection. Error bars are SEM and n is the number of analysed cells.

** indicates p value below 0.001 as compared to WT, as determined by the Mann–Whitney U-test.

Figure S2 - Size of budding sites measured by AFM

(A) Size distribution of HIV-1 Gag-GFP particles. Height and diameter of GFP-positive buds were measured by AFM (n = 60, number of cells = 15). The line represents the linear regression between these 2 parameters.

(B) Distribution of CD9 “true” density in Gag-GFP domains (Gag+) compared to regions of the membrane where Gag-GFP protein is absent (control). The true density is the number of CD9 dSTORM localizations divided by the bud membrane area, measured from AFM topographic images. The control distribution is calculated from areas randomly selected in membrane regions devoid of Gag-GFP (n = 53); these densities were calculated from a 3 pixels x 3 pixels ROI, which is the range of the bud area.

Figure S3 - Correlative images of budding sites

(A) Panel of six representative images of budding sites in different cells expressing Gag-GFP (670 nm x 670 nm zooms): first row, AFM topography images; second row, AFM signal is overlaid with CD9 dSTORM localizations (red dots); third row, idem with GFP-Gag signal in addition (green). The color scale bar for AFM is 350 nm.

(B) Distribution of relative distances between CD9 localizations and the plasma membrane, measured from buds lying on the side of cells. Distances were normalized by the distance from bud tip to plasma membrane and compiled from 12 buds. The image on the left is a representative example of selected CD9 localizations within three buds (cyan, magenta and green) and the segments used to define the plasma membrane for distance measurements. Each bud was divided in 10 slices of equal width and the surface of each slice was measured from the AFM images using Delaunay triangulation (see material and methods) and the bud. The box and whiskers plot represents CD9 density (number of localization / μm^2 extracted from the correlated STORM images). In order to better visualize the wide range of data, we have used a two segments X axis.

Figure S4 - Gag reduces tetraspanin levels at the cell surface of HeLa cells and is not due to intracellular internalization of the proteins

Confocal images of HeLa expressing Gag-GFP proteins. CD9 and CD81 were labeled by indirect immunofluorescence from permeabilized cells. The dash lines indicate the z profile shown at the

bottom. White stars indicate cells expressing Gag-GFP. Scale bar is 10 μm (in x, y and z). The inset corresponds to GM130 labeling to control the permeabilization efficiency.

Figure S5 - CD9 and CD81 are dispensable for VLPs release

The acute enrichment of CD9 and CD81 into Gag-induced budding sites questioned about the functional role of CD9 and CD81 in membrane remodeling and/or bud fission. Since tetraspanins share a number of interactors, CD9 and CD81 may be at least partially redundant, we thus co-depleted CD9 and CD81 by siRNA approach and measured VLP production as well as CD9 and CD81 expression within both cells and VLPs.

A) Cells were co-transfected or not (control - Ctl) with Gag (pNL4-3 Δ) and siRNA targeting CD9, CD81, both tetraspanins or scrambled (Sc) SiRNA. Expression of p24, CD9 and CD81 were analyzed by western blotting. The supernatant is representative of VLP particles released in the extracellular medium. Brackets highlight the expression of CD81 and CD9 when downregulating CD9 and CD81, respectively.

B) Relative expression of CD9 (white box) and CD81 (grey box) in supernatants as compared to control cells (scrambled SiRNA). No significant difference were observed in cell extracts. Importantly no significant difference in p24 expression was observed in both cell extracts and supernatants. Quantitation was performed with FIJI from three independent experiments. Statistical analysis was done in Prism using ANOVA test combined with a Tukey's multiple comparison test; * indicates a p value below 0.05.

Figure S6 - Gag proteins recruit and reorganize the tetraspanin CD81 at the plasma membrane of HeLa cells

(A) dSTORM images of CD81 in a naïve HeLa cell (top) and a Gag-GFP expressing HeLa cell at 48h post-transfection (down) with regions in white boxes (10 μm \times 10 μm) enlarged on the second

column. Scale bars are 5 μm (first column) and 1 μm (second column). Cells boundaries are shown with white dashed line.

(B) CD81 density (number of localization/ μm^2) in control cells (red) or in cells expressing Gag-GFP proteins 48h (green) after transfection.

(C) Histograms representing the CD81 cluster size in nm^2 in WT cells (red) or GFP-Gag-expressing cells 48 h after transfection (green). In the mirror histograms below the X axis, empty and hatched histograms represent the density outside and within Gag-GFP positive areas, respectively. *** indicates a p value below 0.0001 for comparison of CD81 cluster sizes inside Gag domains versus cluster sizes outside these domains, as determined by the Mann-Whitney U-test.

Table S1: CD9 density

| | wt | Gag-24h | | Gag-48h | |
|-------------------|---|-----------|----------------------|---------------------------|------------------------|
| Mean ± sem | 1192 ± 127 | 793 ± 141 | | 658 ± 151 | |
| p-values | 0.0141* 0.0004** | 0.0141 | | 0.0004 | |
| | | Out | In | Out | In |
| Mean | | 748 | 6073 | 429 | 8430 |
| ± | | ± | ± | ± | ± |
| SEM | | 161 | 1387 | 63 | 1655 |
| p-values | 0.0032* <0.0001*** <0.0001*** <0.0001*** | 0.0032 | 0.0003 0.0004 | <0.0001 <0.0001*** | <0.0001 <0.0001 |
| | | 0.0004** | 0.2812 | | 0,2812 |

CD9 density is expressed as the number of localization events per μm^2 (\pm sem). p values were calculated using a non parametric two-tailed Mann-Whitney U-test. *, **, and *** respectively indicate p values below 0.05, 0,001 and 0.0001. Each p value corresponding to a pair of data sets is indicated twice on the same line in the corresponding data set column.

Table S2: CD9 cluster sizes

| | wt | Gag-24h | | Gag-48h | |
|-------------------|--------------------------|-----------------------|-------------------|--------------------|--------------------|
| Mean ± sem | 3710 ± 1513 | 4428 ± 1606 | | 5471 ± 2198 | |
| Max | 248100 | 244551 | | 163721 | |
| Median | 1603 | 2519 | | 2976 | |
| p-values | <0.0001*** <0.0001*** | <0.0001 <0.0001*** | | <0.0001 <0.0001 | |
| | wt | Out | In | Out | In |
| Mean ± sem | 3710 ± 1513 | 4378 ± 1586 | 4423 ± 1648 | 4737 ± 1670 | 6527 ± 2763 |
| Max | 248100 | 244551 | 144715 | 92393 | 163721 |
| Median | 1603 | 2519 | 2519 | 2748 | 3320 |
| p-values | <0.0001*** <0.0001*** | 0.8453 | <0.0001 0.8453 | <0.0001*** | <0.0001 <0.0001 |

CD9 cluster size is expressed in nm² (± sem). p values were calculated using a non parametric two-tailed Mann-Whitney U-test. *, **, and *** respectively indicate p values below 0.05, 0,001 and 0.0001. Each p value corresponding to a pair of data sets is indicated twice on the same line in the corresponding data set column.

Table S4: Correlation between GFP-Gag intensity and CD9 density (Kendall method)

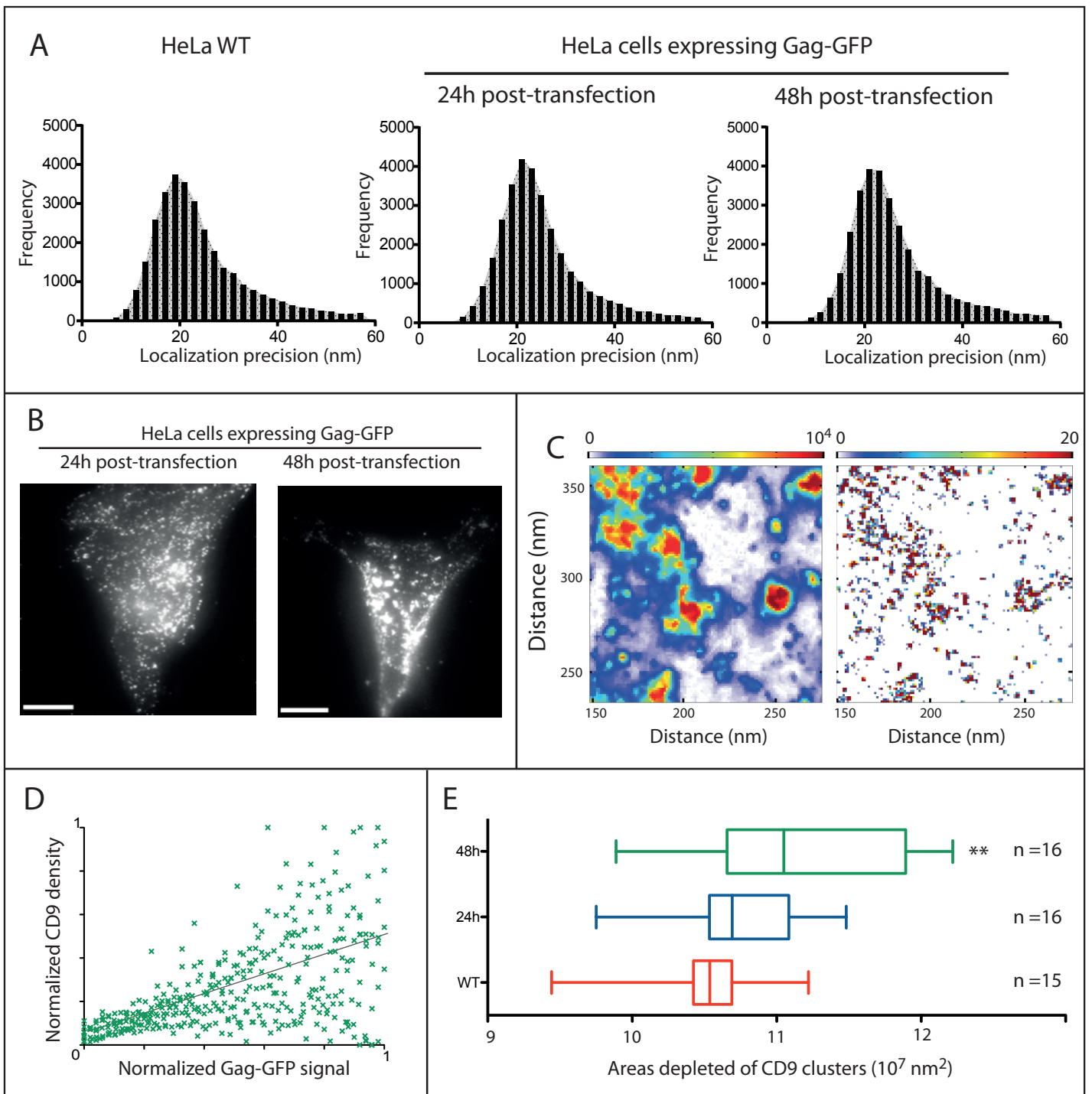
| Cell number | Tau | p-value |
|-------------|------|--------------|
| 1 | 0.73 | 3.10^{-15} |
| 2 | 0.19 | 0.047 |
| 3 | 0.72 | 3.10^{-15} |
| 4 | 0.61 | 5.10^{-10} |
| 5 | 0.85 | 2.10^{-16} |
| 6 | 0.46 | 2.10^{-6} |
| 7 | 0.34 | 0.00066 |
| 8 | 0.57 | 8.10^{-10} |

Bibliography

1 C. Chamontin, P. Rassam, M. Ferrer, P.-J. Racine, A. Neyret, S. Lainé, P.-E. Milhiet and M. Mougel, *Nucleic Acids Res.*, 2015, **43**, 336–347.

2 S. Nydegger, M. Foti, A. Derdowski, P. Spearman and M. Thali, *Traffic*, 2003, **4**, 902–910.

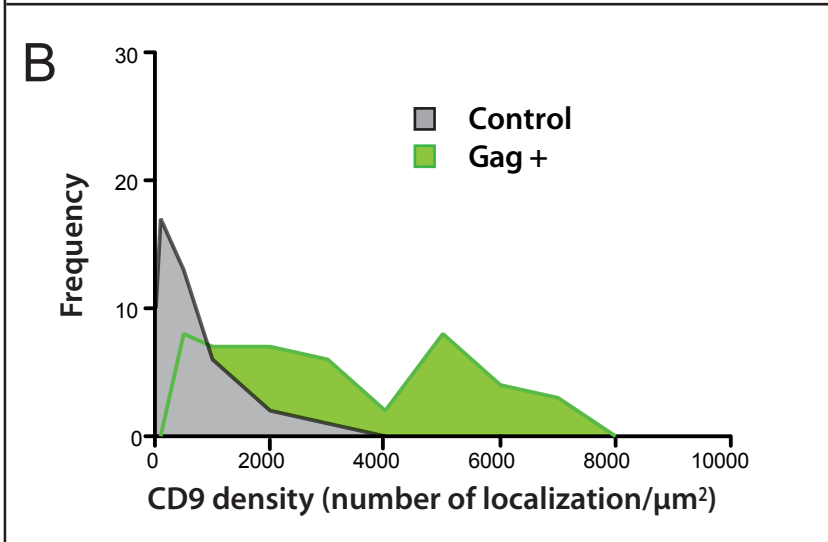
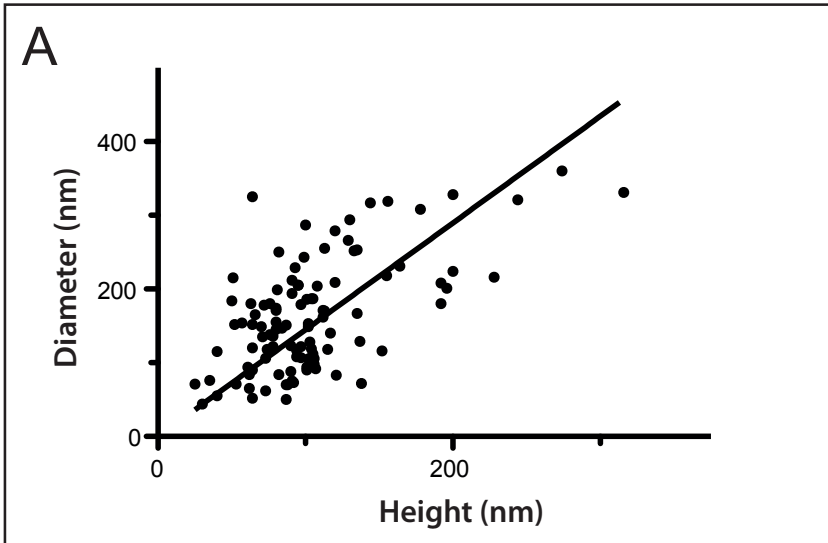
- 3 C. Espenel, E. Margeat, P. Dosset, C. Arduise, C. Le Grimellec, C. A. Royer, C. Boucheix, E. Rubinstein and P.-E. Milhiet, *J. Cell Biol.*, 2008, **182**, 765–776.
- 4 A. Sergé, N. Bertaux, H. Rigneault and D. Marguet, *Nat Meth*, 2008, **5**, 687–694.
- 5 J.-B. Fiche, D. I. Cattoni, N. Diekmann, J. M. Langerak, C. Clerte, C. A. Royer, E. Margeat, T. Doan and M. Nöllmann, *PLoS Biol.*, 2013, **11**, e1001557.
- 6 F. Levet, E. Hosy, A. Kechkar, C. Butler, A. Beghin, D. Choquet and J.-B. Sibarita, *Nat. Methods*, 2015, **12**, 1065–1071.

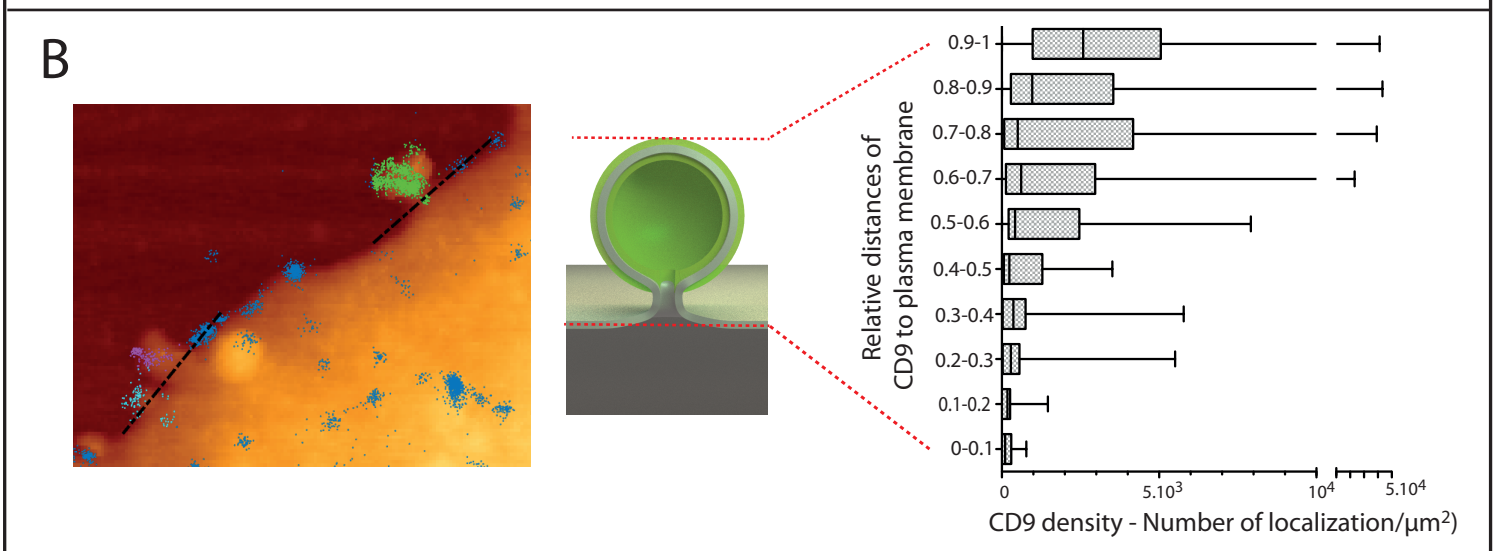
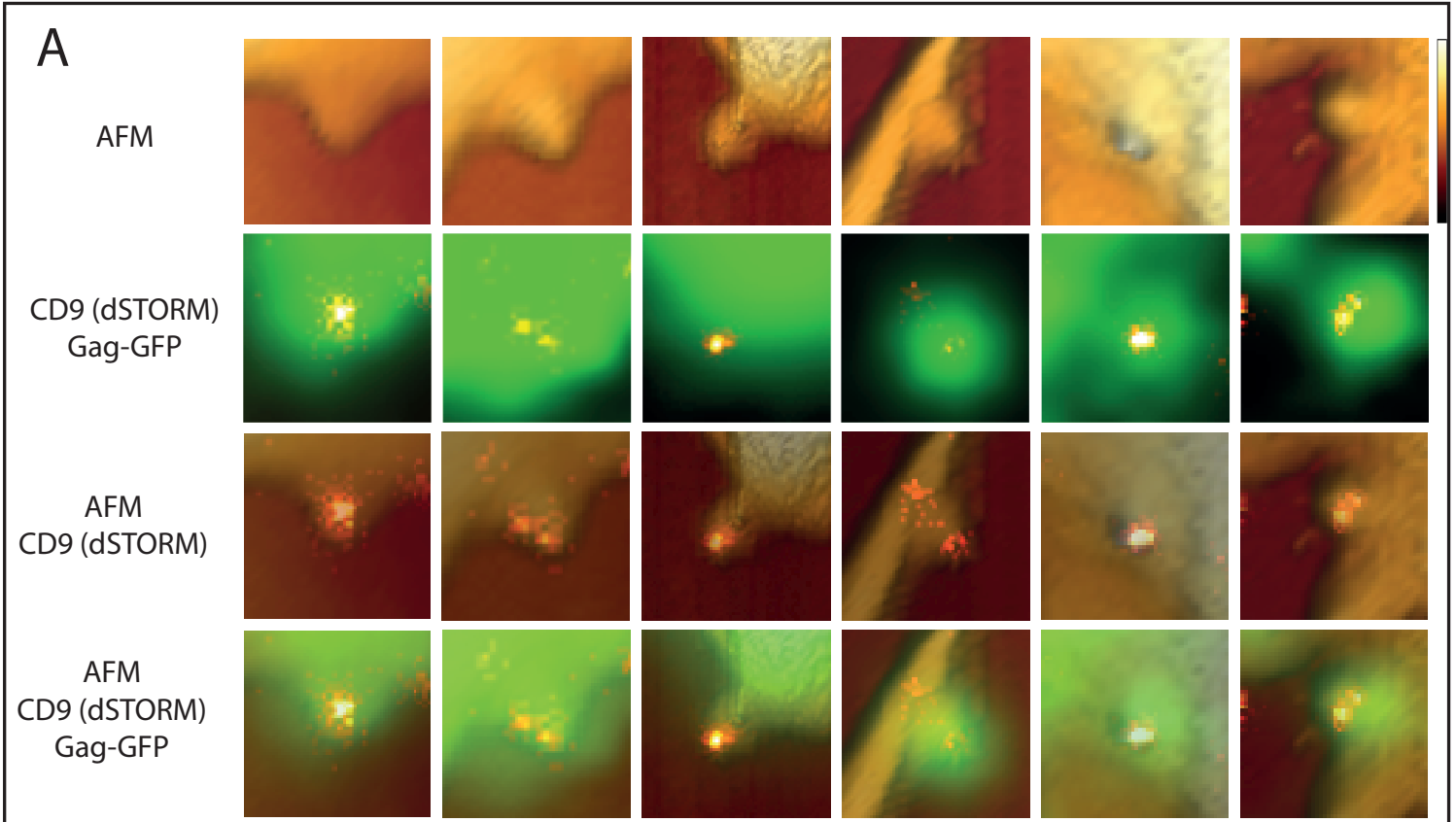


HeLa cells expressing Gag-GFP

24h post-transfection

48h post-transfection





Tetraspanin + Gag

Tetraspanin

